Mixed One-way and Two-way Ranging to Support Terrestrial Alternative Position Navigation & Timing

Jiangping Chu, *Stanford University*

BIOGRAPHY

Jiangping Chu received her M.S. degree from the Department of Aeronautics and Astronautics at Stanford University in 2012. She graduated with a B.S. degree in Mechanical Engineering from Shanghai Jiao Tong University and a B.S. degree in Aerospace Engineering from University of Michigan Ann Arbor in 2010. She was doing research work in the GPS Research Laboratory at Stanford University under the guidance of Prof. Per Enge and Dr. Sherman Lo. Her research interests include alternative position navigation and timing (APNT) and ground-based backup systems to GNSS.

ABSTRACT

Two-way ranging between the ground station and aircraft can provide true-range measurement allowing for horizontal positioning using only two stations. However, this infrastructure benefit comes at a cost, as the two-way ranging requires interaction between ground station and aircraft, which limits system capacity. In this respect, one-way ranging which provides pseudo-range measurement works well because it has no capacity limitations. Its drawback is that we need one extra measurement to solve for the horizontal position and clock offset. In this paper, we look at positioning using mixed one-way and two-way ranging, which can work in limited geometry situation while having a high system capacity.

In mixed positioning, two modes are considered: 1) clock calibration and 2) clock coasting mode. In clock calibration mode, determination of the airborne user clock offset is made as the clock offset may be unknown or exceed some targeted threshold. To achieve the calibration, at least three measurements are needed to estimate the horizontal position and clock offset. Calibration of the clock allows for clock-coasting mode where the horizontal position can be determined with fewer measurements through coasting with the previously determined clock offset. In this mode, only two pseudo-range measurements are required to navigate the aircraft. However, one must take care as the uncertainty of the clock offset will grow as time increases. The error growth speed depends on clock precision of the onboard clock.

For the aircraft navigation, integrity must be considered. Generally, under reasonable geometry, at least three measurements are needed to estimate the horizontal position of the aircraft and clock offset. One more measurement is necessary for detecting a faulty measurement source, and if additional measurements are available, it is possible to isolate the faulty measurement source.

This paper details how the measurement errors effect on horizontal positioning and clock offset by examining different cases using one-way and possibly two-way ranges. With the knowledge of these initial measurement uncertainties, it is possible to obtain the allowable coasting time within which the system can meet the requirements without clock update. Moreover, this paper utilizes a classical method to detect the faulty measurement source using one redundant range measurement to examine mixed ranging integrity and the effect of clock offset.

1. INTRODUCTION

The Federal Aviation Administration (FAA) is initiating the Alternative Position Navigation and Timing (APNT) program to develop system(s) that can minimize the impact of a degradation of the Global Positioning System (GPS) and other Global Navigation Satellite Systems (GNSS). The APNT program will develop a system capable of maintaining efficient and safe operations even in the absence of GPS. This system will leverage existing FAA terrestrial infrastructure and signals for robust operations [1][2]. The APNT solution is expected to be able to support the horizontal positioning for key operational capabilities in en route and terminal airspace while maintaining full system capacity. These are difficult and contrasting goals, especially for the terminal area, as fewer terrestrial ground stations are visible to aircraft at the lower altitudes used in terminal airspace while high capacity prefers more stations.

Two-way ranging systems, such as distance measuring equipment (DME), make the best use of stations available as they provide true-range measurements allowing for horizontal positioning using only two stations. However, this infrastructure benefit comes at a cost, as the two-way measurement requires interaction between ground station and aircraft, which limits system capacity [3]. One-way ranging (passive ranging) provides pseudo-range measurements and needs an additional station for positioning, but has no capacity limitations. This paper focuses on a mixed or hybrid positioning method for horizontal positioning using both one-way and two-way measurements to provide operations in limited geometry situation while having high system capacity. Such an architecture is reasonable when a site can supply both forms of ranging.

Mixed positioning makes sense for APNT from an infrastructure perspective. APNT will leverage existing FAA terrestrial infrastructure such as DME and ground based transceiver (GBT) sites. These sites may support both forms of ranging signals or they can accommodate multiple transmitter such that there is both a one-way and two-way ranging signal. Having the infrastructure benefit is important as APNT needs the most accuracy in terminal airspace where there are fewer sites visible due to proximity to the ground. These are also typically the most congested airspaces. Furthermore, additional infrastructure will need to be justified from a cost-benefit perspective.

OUTLINE

This paper begins by examining the two primary modes of operation in mixed or hybrid positioning: 1) clock calibration and 2) clock coasting. In the first mode, a determination of the position solution and the airborne user clock offset relative to the ground infrastructure (the ground is assumed to be on a common clock) is made. This is needed as the aircraft clock offset may be unknown or exceed some targeted threshold. To achieve the calibration, at least three measurements are needed to estimate the current horizontal position and clock offset. The second mode utilizes the previously determined clock offset to coast and perform a position solution with fewer measurements. In this case, only two pseudo-range measurements are required to navigate the aircraft. In this way, clock-coasting mode can minimize the required amount of ground stations for APNT. However, one must be cautious as the uncertainty of the clock offset represents a potential integrity risk.

This paper then considers integrity and fault detection. Generally, under reasonable geometry, without the clock offset, at least three measurements are needed to estimate the horizontal position of the aircraft and clock offset. An additional measurement is necessary for detecting one faulty measurement source, with further measurements allowing for detection of the faulty measurement source. This paper applies a classical method of integrity monitoring in the aircraft navigation to mixed positioning.

2. BACKGROUND

The APNT program is examining several key technologies. One candidate is DME that currently provides en route coverage and is equipment on many aircrafts. Another candidate is terrestrial passive ranging system ("pseudolite") that can provide unlimited capacity and potentially new services.

DME system is a two-way ranging system whereby the aircraft determines its distance or true range from a ground-based DME transponder by sending (interrogation) and receiving (reply) pulse pairs. As each DME range measurement requires an interaction between aircraft and station to provide a true-range measurement, DME system is capacity limited. Using this system, two DME ranges (i.e. true ranges) will be enough for horizontal positioning. Scanning DME or DME/DME avionics onboard the aircraft is able to interrogate multiple DME transponders near simultaneously to determine position.

APNT is also examining passive ranging or pseudolite technologies. Note that APNT uses the term pseudolite to generically refer to any terrestrial passive ranging system, not necessarily GPS-like system. One benefit of this system is its unlimited system capacity. Another benefit is data. Many of the pseudolite options can also support reasonable amounts of data providing a means to provide security, robustness, integrity messaging and other value added benefits. But using only pseudo-range measurements, at least three measurements are required to estimate the horizontal position and clock offset. This means that a pseudolite system needs one more station than a true ranging system. It also needs the ground stations to be reasonably synchronized.

Some pseudolite technologies for passive ranging system being examined by APNT include: DME based passive ranging (DMPR), universal access transceiver (UAT)[5], aviation transponder broadcasts (1090 MHz), L band digital aviation communication systems (LDACS)[8] and Ultra High Accuracy Reference System (UHARS)[7]. DMPR uses standard DME pulse pairs to create a passive ranging and data signal. The design was created to be compatible with and have minimal impact on existing, nominal DME operations [4][5]. UAT is one of two signals being implemented to support automatic dependent surveillance broadcast (ADS-B). APNT is examining the use of the pseudo-ranging capabilities built into the ground segment signal transmitted from GBT. These signals can also be transmitted on a DME beacon antenna

as they are located an unused portion of the DME band. Transponder transmissions are used by secondary surveillance radar (SSR) to determine range to and other information about an aircraft. Additionally, Mode S extended squitter on the 1090 MHz transponder frequency also supports ADS-B.

The pseudolite developments make mixed positioning an attractive option as the same source may provide both one-way and two-way ranging. For example, an improved DME system will be able to provide both one-way and two-way ranging through DMPR and traditional DME operations. Similarly, UAT currently can provide passive ranging in its ground segment transmissions. In its ADS-B segment, a two-way transmission such as an interrogation-reply may be possible. Hence with many of these sites, both one-way and two-way ranging is possible allowing geometry and capacity benefits. However, mixed ranging will require carriage of a clock that will allow the aircraft to operate with one-way (passive) ranging signals only for a reasonable period of time while meeting accuracy requirements.

RANGING ERROR ASSUMPTIONS

Ranging errors depend on the source and type of the signal used – for example DME and DMPR or UAT pseudo and true ranging. In the paper, we derive generic results. However, in the analysis, we want to provide a sense of the actual performance as so this section discusses the basis for some of the values used. Previous analysis assessed the ranging capabilities of some of these systems[4][5]. Based on those results, we can make some conservative assumptions the range measurement errors excluding multipath. The expected value of the DMPR and UAT pseudo-range measurement error is 10 meters (1 sigma). For two-way ranges, two measurements of time are made and so, simplistically, the error in calculating travel time is roughly doubled that of the one-way. However, the range calculation divides this travel time by two is it is effectively the same level of error. In DME, as the pulse shape from the aircraft is generally not as well controlled as that from the ground, one would expect more errors on the measurement of the signal from the aircraft. Hence, for true range, we use an expected value of the true-range measurement errors is 20 meters (1 sigma). As the transmission up from the ground transmitter to the aircraft should be similar for both ranging methods, we assume a correlation between the one-way and two-way ranges from a station to be 0.5.

CLOCK PERFORMANCE

A basic model for clocks was used to estimate the performance of representative clock technologies and their impact on a mixed ranging system for APNT.

Table 1 shows the stability and aging performance for five different oscillator classes: crystal oscillator (XO), temperature compensated crystal oscillator (TCXO), oven controlled crystal oscillator (OCXO), Rubidium-crystal oscillator (RbXO), and Cesium oscillator (Cs).

Eqn. 1 shows the equation used to derive clock offset over time [9]. Some simplifying assumptions are made: 1) zero drift and 2) constant $\sigma_y(t)$. The $\sigma_y(t)$ used is based on the one second value. Zero drift implies that clock frequency has been recently calibrated. This is reasonable to conservative for up to about 100 seconds for Quartz oscillator and much longer (1000 seconds or more) for atomic standards[9]. Furthermore, the parameters used (aging,) are rough and can vary from model to model. However, the analysis is reasonable as the goal is to get an order of magnitude estimate of performance levels and determine minimum clock type needed.

Accuracy per year values in the table can be used which accounts for environmental effects and one year of aging. **Eqn. 2** shows the calculation that expresses the long-term stability of the oscillator (one that has not been calibrated for some time). One would expect the result to be conservative as GPS, when available, may be used to calibrate the oscillator.

$$t_{err}(t) = t_{err}(0) + drift * t + \tfrac{1}{2} aging * t^2 + \int_0^t \sigma_y(t)\, dt$$

Equation 1: Clock Offset Over Time

$$t_{err}(t) = Accuarcy * t$$

Equation 2: Clock Offset from Accuracy/Year value

Table 1: Stability and Aging Performance for Different Oscillator Classes (based on [9] [12])

	Crystal Oscillators (XO)			Atomic Oscillators	
	XO	TCXO	OCXO	RbXO	Cesium
Accuracy (per year)	$1x10^{-4}$ to $1x10^{-5}$ [12]	1×10^{-6} [12]	1×10^{-8}	$7x10^{-10}$	$2x10^{-11}$
Stability,σ_y (τ), 1 sec	$2x10^{-7}$	$1x10^{-9}$	$1x10^{-12}$	$5x10^{-12}$	$5x10^{-11}$
Aging/year	$1x10^{-6}$	$5x10^{-7}$	$2x10^{-7}$	$1x10^{-12}$	0

ACCURACY REQUIREMENTS

The accuracy requirement derives from the APNT performance target of supporting operations in terminal airspace. Specifically targeted navigation capabilities are Area Navigation (RNAV) 0.3 and required navigation performance (RNP) 0.3 which have total system error (TSE) accuracy requirements of 0.3 nautical miles (nm). APNT also seeks to support surveillance for three-nautical mile separation. **Table 2** derives the targeted signal ranging accuracy applicable for one-way and two-way ranging systems. It uses the position accuracy

requirements of the targeted operations, assumed worst case horizontal dilution of precision (HDOP) of 2.828, and a time synchronization accuracy of 50 ns. Additionally, a flight technical error (FTE) of 0.25 nm, as specified in DO-208 for flight director [6], is assumed for RNP/RNAV resulting in the navigation system accuracy of 307.2 m and 1793 m. Surveillance is considering requiring a navigation accuracy (2 sigma) of 92.6 m or 0.05 nm to support three-mile separation.

Table 2: Accuracy Requirements for Navigation and Surveillance

Operation	Navigation System accuracy	Range accuracy (HDOP 2.8)	Time accuracy (estimated)	Implied signal accuracy
RNAV/RNP 0.3	307.2 m	108.6 m	50 ns (15 m)	107.5 m
RNAV/RNP 1.0	1793 m	634.0 m	50 ns (15 m)	633.8 m
Surveillance	92.6 m	32.7 m	50 ns (15 m)	29.1 m

3. CLOCK CALIBRATION

Fig. 1 shows the two modes used for mixed positioning: 1) clock calibration and 2) clock coasting mode. This section discusses the first mode in detail on the effect of different types of measurement errors. The study is conducted by theoretical analysis.

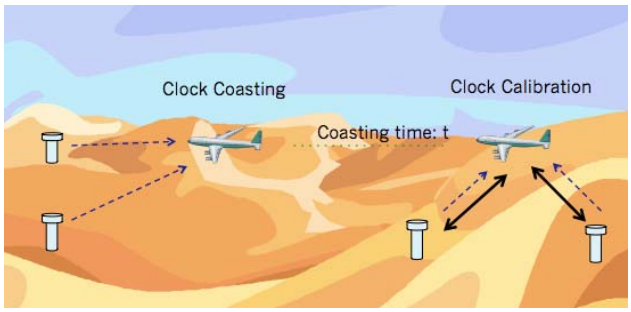

Figure 1: Two Modes in Mixed Positioning

In clock calibration mode, the airborne user clock offset relative to the ground stations (which are synchronized) is unknown or exceeds some targeted threshold. As a result, clock offset needs to be estimated from the measurements, which requires at least three measurements for three unknowns: clock offset and horizontal position.

The calibration can be achieved with two pseudo-range measurements and one true-range measurement (perfect-determined scenario) or two pseudo-range measurements and two true-range measurements (over-determined scenario), where the true-range measurements can be taken from the pseudo-range sources. This section discusses these two scenarios in detail to study how different types of measurement errors affect the estimation of clock offset. The redundant measurement in the over-determined scenario can be used to detect a faulty source, which will be discussed in later section.

MEASUREMENT ERROR ANALYSIS

Several cases of measurement errors are studied in clock calibration mode. These are:

- Unbiased, independent identically distributed (i.i.d)
  $\varepsilon \sim N[0,\sigma]$
- i.i.d with one biased/faulty measurement
  $\varepsilon_1 \sim N[\mu_1,\sigma]$, $\varepsilon_i \sim N[0,\sigma]$ for $i \neq 1$
- Independent, biased measurements
  $\varepsilon_i \sim N[\mu_i,\sigma_i]$
- Correlated (same site), biased measurements
  $\varepsilon_i \sim N[\mu_i,\sigma_i]$

The first case has no bias in all the measurements and all the measurement errors are independent and identically distributed (i.i.d) with the same variance, σ^2. The second case also has i.i.d errors with the same variance with the exception that the one of the measurements has bias. In the last two cases, all the measurement errors have different bias and different variances. This results in use of a weighted solution based on these different variances. For correlated case, correlation coefficient, ρ, defined in **Eqn. 3**, is used to describe the covariance of two measurements such as the one-way and two-way ranges from a given transmitter. (Correlation between signals from the same station)

$$\rho_{XY} = \frac{Cov(X,Y)}{\sigma_X \sigma_Y}$$

Equation 3: Definition of Correlation Coefficient

PERFECT-DETERMINED SCENARIO (UNIQUELY-DETERMINED)

For perfect-determined problem, we have exactly three measurements to solve for three unknowns. Here, two pseudo-range measurements and one true-range measurement are used to estimate the horizontal position and clock offset, where the true-range measurement is taken from one of the pseudo-range sources, so two stations are required in this scenario.

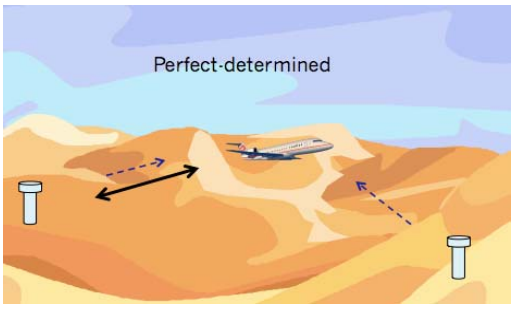

Figure 2: One True-range and Two Pseudo-range Measurements

First, to setup the system coordinate, the current position of aircraft is set as the origin, while the line connecting aircraft and one of the stations is x-axis.

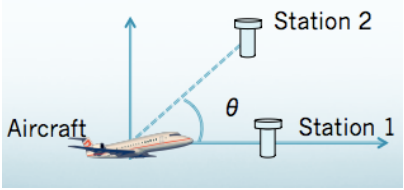

Figure 3: System Coordinate Setup

In this coordinate, the geometry matrix can be written as:

$$\boldsymbol{G} = \begin{matrix} \mathbf{1} & \mathbf{0} & \mathbf{0} \\ \mathbf{1} & \mathbf{0} & \mathbf{1} \\ \boldsymbol{\cos\theta} & \boldsymbol{\sin\theta} & \mathbf{1} \end{matrix}$$

$$\tilde{z} = \begin{matrix} R_1 \\ \rho_1 \\ \rho_2 \end{matrix}, \tilde{x} = \begin{matrix} x \\ y \\ b \end{matrix}$$

where $\tilde{\boldsymbol{z}} = \boldsymbol{G}\,\tilde{\boldsymbol{x}} + \boldsymbol{\varepsilon}$, $\tilde{\boldsymbol{z}}$ is the measurement vector including one true-range measurement and two pseudo-range measurements, $\tilde{\boldsymbol{x}}$ is the unknown vector including horizontal position (x,y) and clock offset (b), and $\boldsymbol{\varepsilon}$ is the error vector.

Using traditional analysis methods: least-square method and weighted least-square method for the weighted cases to get the estimated position and clock offset:

$$\hat{x} = (G^T G)^{-1} G^T \tilde{z}$$

Equation 4: Least-Square Method to Estimate Horizontal Position and Clock Offset

or for weighted cases:

$$\hat{x} = (G^T wG)^{-1} G^T w\tilde{z}$$

Equation 5: Weighted Least-Square Method to Estimate Horizontal Position and Clock Offset

$$\delta\hat{x} = (G^T G)^{-1} G^T \varepsilon$$

Equation 6: Least-Square Method to Estimate Errors

or for weighted cases:

$$\delta\hat{x} = (G^T wG)^{-1} G^T w\varepsilon$$

Equation 7: Weighted Least-Square Method to Estimate Errors

where $\delta\hat{x} = \hat{x} - \tilde{x}$, is the difference between the actual and estimated position and clock offset.

Therefore, the uncertainties of the estimated horizontal position and clock offset can be obtained by the equations below:

The expected value, $E[\delta\hat{x}] = (G^T G)^{-1} G^T E[\varepsilon]$

Or for weighted cases: $E[\delta\hat{x}] = (G^T wG)^{-1} G^T wE[\varepsilon]$.

The covariance matrix for measurement errors of i.i.d. can be obtained by:

$$Cov[\tilde{x}] = \sigma^2 (G^T G)^{-1}$$

Equation 8: Covariance Matrix of Estimation for i.i.d Errors

Where σ^2 is the identical variance for all measurement errors.

Or for weighted cases:

$$Cov[\delta\hat{x}] = (G^T wG)^{-1} G^T w\, Cov[\varepsilon][(G^T wG)^{-1} G^T w]^T = (G^T wG)^{-1}$$

Equation 9: Covariance Matrix of Estimation for Weighted Cases

The effect of different types of measurement errors on the calibration can be found and shown in **Table 3.**

OVER-DETERMINED SCENARIO

In the over-determined scenario, two true-range measurements and two pseudo-range measurements are used to estimate the horizontal position and clock offset. Two stations are enough and studied in this scenario, with each station providing one true-range and one pseudo-range measurements. Note that more stations can be used to provide a solution that is over-determined by one measurement: 1) Four providing pseudo-ranges, 2) Two stations providing pseudo-ranges and one station providing both pseudo-range and true-range.

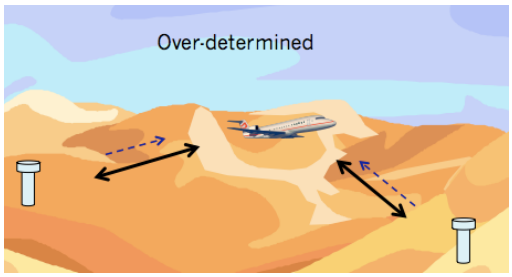

Figure 4: Two pseudo-range and Two true-range Measurements

The setup of the system coordinate is the same as perfect-determined scenario. The geometry matrix is a 4 by 3 matrix, which can be found as:

$$G = \begin{matrix} 1 & 0 & 0 \\ 1 & 0 & 1 \\ \cos\theta & \sin\theta & 0 \\ \cos\theta & \sin\theta & 1 \end{matrix}$$

$$\tilde{z} = \begin{matrix} R_1 \\ \rho_1 \\ R_2 \\ \rho_2 \end{matrix}, \tilde{x} = \begin{matrix} x \\ y \\ b \end{matrix}$$

where $\tilde{\boldsymbol{z}} = \boldsymbol{G}\,\tilde{\boldsymbol{x}} + \boldsymbol{\varepsilon}$, $\tilde{\boldsymbol{z}}$ is the measurement vector including true-range measurement and pseudo-range measurements from two stations respectively, $\tilde{\boldsymbol{x}}$ is the unknown vector including horizontal position (x,y) and clock offset (b), and $\boldsymbol{\varepsilon}$ is the error vector.

Using the same method as in perfect-determined scenario, the effect of different types of measurement errors on the clock calibration can be found and shown in **Table 4**.

Table 3: Analysis Summary for Perfect-determined Scenario

	Case 1: Three measurements (Perfect-determined)	
	$E[\hat{b}]$	$(\sigma \times TDOP)^2$
$\varepsilon \sim N[0,\sigma]$	0	$2\,\sigma^2$
$\varepsilon \sim N[\mu,\sigma]$ Biased on R_1, identical variance	$-\mu_1$	$2\,\sigma^2$
$\varepsilon \sim N[\mu_i,\sigma_i]$ Biased, weighted, uncorrelated	$\mu_2 - \mu_1$	$\sigma_1^2 + \sigma_2^2$
$\varepsilon \sim N[\mu_i,\sigma_i]$ Biased, weighted, correlated	$\mu_2 - \mu_1$	$\sigma_1^2 + \sigma_2^2 - 2\rho_{12}\sigma_1\sigma_2$

Table 4: Analysis Summary for Over-determined Scenario

	Case 2: Four measurements (Over-determined)	
	$E[\hat{b}]$	$(\sigma \times TDOP)^2$
$\varepsilon \sim N[0,\sigma]$	0	σ^2
$\varepsilon \sim N[\mu,\sigma]$ Biased on R_1, identical variance	$-\frac{\mu_1}{2}$	σ^2
$\varepsilon \sim N[\mu_i,\sigma_i]$ Biased, weighted, uncorrelated	$\frac{-[(\mu_3-\mu_4)(\sigma_1^2+\sigma_2^2)+(\mu_1-\mu_2)(\sigma_3^2+\sigma_4^2)]}{\sigma_1^2+\sigma_2^2+\sigma_3^2+\sigma_4^2}$	$\frac{1}{\frac{1}{\sigma_1^2+\sigma_2^2}+\frac{1}{\sigma_3^2+\sigma_4^2}}$
$\varepsilon \sim N[\mu_i,\sigma_i]$ Biased, weighted, correlated	$\frac{-[(\mu_3-\mu_4)(\sigma_1^2-2\rho_{12}\sigma_1\sigma_2+\sigma_2^2)+(\mu_1-\mu_2)(\sigma_3^2-2\rho_{34}\sigma_3\sigma_4+\sigma_4^2)]}{(\sigma_1^2-2\rho_{12}\sigma_1\sigma_2+\sigma_2^2)+(\sigma_3^2-2\rho_{34}\sigma_3\sigma_4+\sigma_4^2)}$	$\frac{1}{\frac{1}{\sigma_1^2-2\rho_{12}\sigma_1\sigma_2+\sigma_2^2}+\frac{1}{\sigma_3^2-2\rho_{34}\sigma_3\sigma_4+\sigma_4^2}}$

Table 3 and **Table 4** summarize the clock uncertainties in each case. The subscript number indicates which error it represents, like σ_1 represents the standard variation of the error of the first measurement. For the correlated case, we made an assumption that there is no correlation between measurements from different stations, that is, $\rho_{13} = \rho_{23} = \rho_{14} = \rho_{24} = 0$. These results will be used to calculate the initial clock uncertainty in clock coasting mode.

COMPARISON OF HDOP

Table 3 and **Table 4** compare the time dilution of precision (TDOP) for two scenarios. **Fig. 5** compares the HDOP values in two scenarios with the first type of measurement errors: unbiased with identical variance.

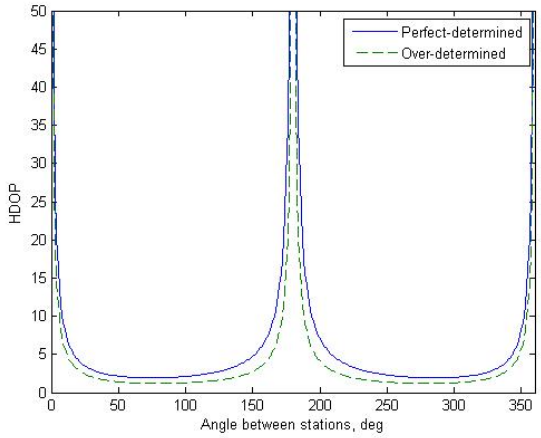

Figure 5: Comparison of Performance on HDOP

The performance on HDOP varies at different geometry. The singular points are at 0, 180 and 360 degrees. The performance is symmetric about 180 degrees. As anticipated, the over-determined scenario has smaller HDOP value, which indicates a better performance.

4. CLOCK COASTING

The results in the clock calibration mode are then used to calculate future positioning solutions. After the aircraft

clock has been calibrated and synchronized to the ground clock, the avionics can directly convert pseudo-ranges to true ranges. Hence two pseudo-range measurements and previously determined clock offset can be used to estimate the current horizontal position. However, the clock offset (aircraft to ground clock synchronization) will grow as time increases due to aircraft clock drift. The error growth speed depends on clock precision of the onboard clock. Given the accuracy requirements, the rough maximal coasting time - that is, how long the aircraft can go without clock update -for each clock class can be determined. This section will examine nominal navigation solution in clock coast mode and the effect of clock offset growth.

CLOCK COAST WITH SYNCHRONIZED CLOCK

With two pseudo-ranges and the calibrated clock, we can formulate the navigation equation to solve for the position solution. Given the navigation equation $\tilde{z} = G\,\tilde{x} + \varepsilon$. Where

$$\tilde{z} = \begin{matrix} \rho_1 \\ \rho_2 \\ t_u \end{matrix}$$

$$G = \begin{bmatrix} 1 & 0 & 1 \\ \cos\theta & \sin\theta & 1 \\ 0 & 0 & 1 \end{bmatrix}$$

ρ_1 and ρ_2 are two pseudo-range measurements, and t_u is the previously determined clock offset.

Assume that the three components of vector ε are all normal distributed, as follows:

$$\varepsilon_{\rho_1} \sim N[\mu_1, \sigma_1],\ \varepsilon_{\rho_2} \sim N[\mu_2, \sigma_2],\ \varepsilon_t \sim N[\mu_3, \sigma_3]$$

Using **Eqn. 9**, we can get the variances of δx, δy and δt with the same assumptions as used to calculate the initial clock uncertainty:

$$\sigma^2[\delta x] = \sigma_1^2 + \sigma_3^2$$

$$\sigma^2[\delta y] = \frac{\cos^2\theta\,{\sigma_1}^2 + {\sigma_2}^2 + (1-\cos\theta)^2{\sigma_3}^2}{\sin^2\theta}$$

$$\sigma^2[\delta t] = {\sigma_3}^2$$

Equation 10: Uncertainties of Errors with Assumptions

$$\text{Horizontal accuracy} = \sigma^2[\delta x] + \sigma^2[\delta y] = \frac{{\sigma_1}^2 + {\sigma_2}^2 + 2\,(1-\cos\theta){\sigma_3}^2}{\sin^2\theta}$$

The contribution of the clock offset in the position domain is then:

$$\sigma^2[\delta x] + \sigma^2[\delta y], \text{from clock} = \frac{2\,(1-\cos\theta){\sigma_3}^2}{\sin^2\theta}$$

Equation 11: Position Errors Contribution from Clock

INITIAL CLOCK UNCERTAINTY

In the clock calibration mode, we determined the aircraft clock offset to the ground and its variance. The resulting clock offset variance using two pseudo-range measurements with one or two true-range measurements from two ground stations are presented in **Table 3** and **Table 4.** The result for the general case with correlation between measurements from the same station is shown below. This provides the initial clock uncertainty.

2 pseudo & 1 true ranges:

$$(\sigma * TDOP)^2 = {\sigma_1}^2 - 2\rho_{12}\sigma_1\sigma_2 + {\sigma_2}^2$$

2 pseudo & 2 true ranges:

$$(\sigma * TDOP)^2 = \frac{1}{\frac{1}{{\sigma_1}^2 - 2\rho_{12}\sigma_1\sigma_2 + {\sigma_2}^2} + \frac{1}{{\sigma_3}^2 - 2\rho_{34}\sigma_3\sigma_4 + {\sigma_4}^2}}$$

Equation 12: Initial Clock Uncertainty

Again we denote σ_1 and σ_2 as the variance of the true-range and pseudo-range measurement errors for Station 1, and σ_3 and σ_4 as the variances for Station 2. Correlations between measurements for a station, ρ_{12} and ρ_{34} are equal to 0.5 based on our assumptions.

ERROR GROWTH MODELING

Figure 6: The Second Stage in Clock Coating Mode

After a certain time, t, the aircraft flies to another position. Using the previously determined clock offset and only two pseudo-range measurements from two stations, we are able to estimate the current horizontal position. In this way, we can minimize the required amount of ground stations at current position. Additionally, we want to propagate the clock offset uncertainty as it will grow as time increases. The error growth rate depends on clock precision of the onboard clock. Therefore, the maximal coasting time, that is, the maximal time the aircraft can go without clock update will be constrained by the given performance requirements.

In this section, an error growth modeling is provided to elaborate the effect of clock-offset error on the variance of horizontal position error. For the initial study, we hold the geometry fixed as the time of interest (seconds to minutes) should only result in a small change in angle relative to the ground stations. Hence, the change of the geometry between two stages due to the aircraft movement is not considered here.

Five types of onboard clocks are discussed: crystal oscillator (XO), temperature compensated crystal oscillator (TCXO), oven controlled crystal oscillator (OCXO), atomic Rubidium-crystal oscillator (RbXO), and atomic Cesium oscillator (Cs).

Given two models for the precision of the onboard clock (Model 1: recently calibrated and Model 2: 1 year of aging), **Fig. 7** and **Fig. 8** shows the rough error growth of the clocks for these models in 180 seconds:

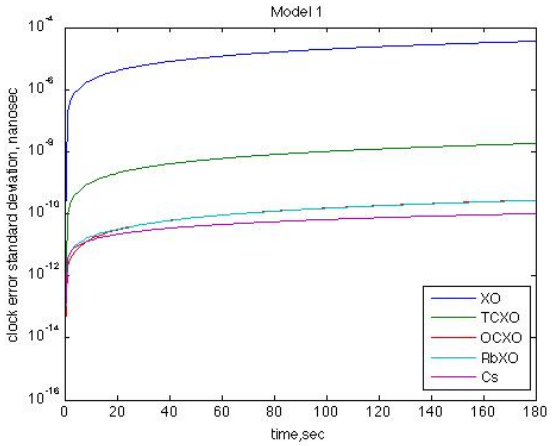

Figure 7: The Rough Error Growth of Onboard Clocks Based on Eqn. 1 for Model 1

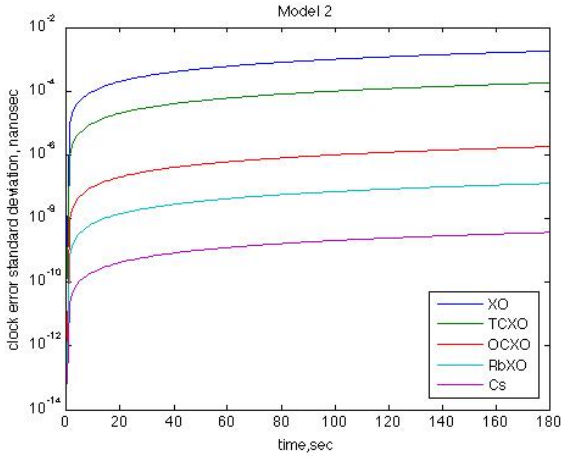

Figure 8: The Rough Error Growth of Onboard Clocks Based on Eqn. 2 for Model 2

Model 2 is a conservative estimate, while Model 1 is a more likely result in reality. In the figures above, the y-axis represents the standard deviation of the total clock offset in nanoseconds (ns), which can be converted to meters with 3 meters equaling 10 ns.

Given the initial clock uncertainty and the model for clock offset variance for different onboard clocks, we are able to model the total position error growth.

The effect of the clock offset on position errors depends on the geometry of the stations as seen in **Eqn. 11**. **Eqn. 13** shows how the clock offset grows in time using the clock offset growth shown in the previous figures. Taking $\theta = 80$ degrees as a special case, the relation between variance of total position error and time increment is shown in **Fig. 9** and **Fig. 10.**

$$\sigma_{clk}{}^2(t) = \sigma_{clk,initial}{}^2 + \sigma_{clk\ err\ growth}{}^2(t)$$

Equation 13: Clock Offset Growth Model

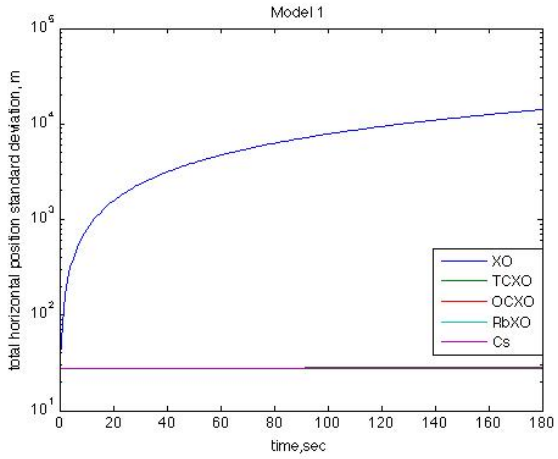

Figure 9: Error Growth Modeling at an 80 degree Offset between Stations (Model 1) using Eqn. 10

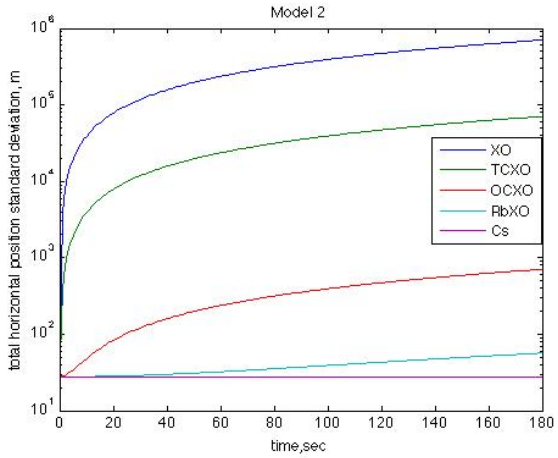

Figure 10: Error Growth Modeling at an 80 degree Offset between Stations (Model 2) using Eqn. 10

If given the performance requirements, like an upper bound of the total position error variance, we will be able to find the maximal coasting time the aircraft can go without clock update. The maximal coasting time varies for different types of clocks.

The maximal coasting time also depends on the geometry of ground stations. The performance will be symmetric about 180 degrees, and the singular point of geometry matrix is at 0 or 180 degrees. The following figures (Fig. 11 to 14) show the maximal time for different types of onboard clocks versus different geometries (20 to 160 degrees).

The subplots are ordered as: XO, TCXO, OCXO, RbXO, Cs. Note that, we only consider the error growth within 3 minutes (180 seconds), which means that if the solved maximal coasting time is 180 seconds, the performance meets the requirement and the aircraft can go without clock update for at least 180 seconds.

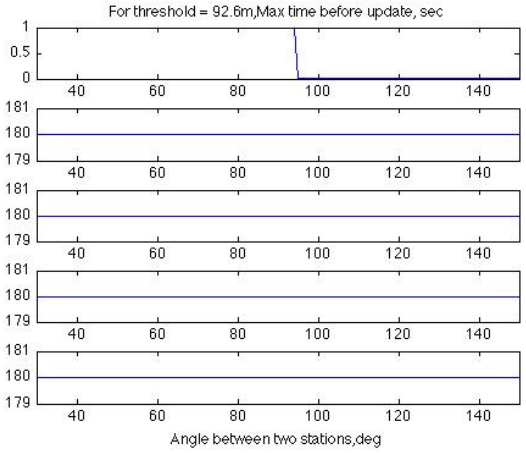

Figure 11: For Threshold 92.6m, the Maximal Coasting Time for Different Clocks over Different Geometries Using Model 1 (Position Domain)

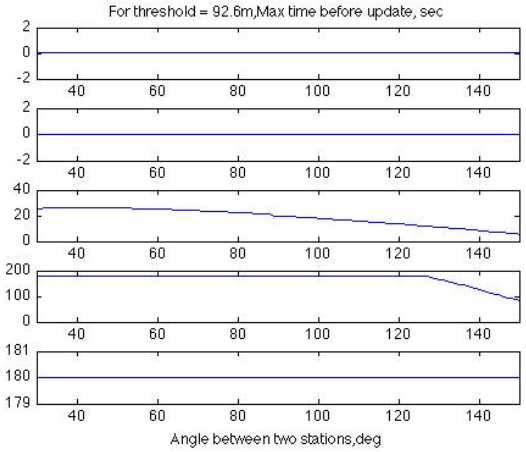

Figure 12: For Threshold 92.6m, the Maximal Coasting Time for Different Clocks over Different Geometries Using Model 2 (Position Domain)

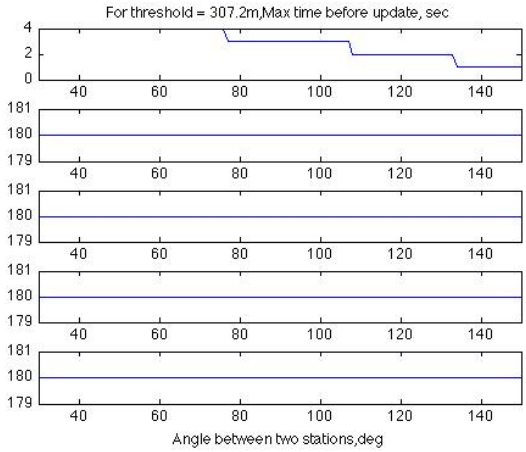

Figure 13: For Threshold 307.2 m, the Maximal Coasting Time for Different Clocks over Different Geometries Using Model 1 (Position Domain)

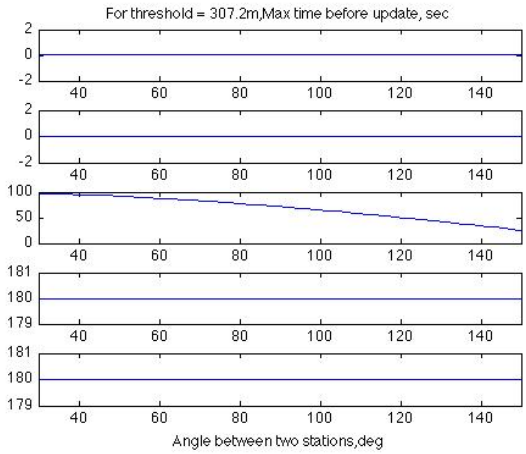

Figure 14: For Threshold 307.2m, the Maximal Coasting Time for Different Clocks over Different Geometries Using Model 2 (Position Domain)

The table below summarizes the maximal coasting time for different types of clocks.

Table 5: Maximal Coasting Time for Different Clocks

Maximal Coasting_Time (Second)	Model 1 (Recently Calibrated)		Model 2 (One Year of Aging)	
Threshold	92.6m	307.2m	92.6m	307.2m
XO	<1	1~4	$<10^{-5}$	$<10^{-5}$
TCXO	>180	>180	$<10^{-5}$	$<10^{-5}$
OCXO	>180	>180	5~25	25~97
RbXO	>180	>180	>81	>180
Cs	>180	>180	>180	>180

5. INTEGRITY

In aircraft navigation, integrity must be considered. In this section, navigation system integrity monitoring using one redundant measurement will be briefly discussed. One redundant measurement is necessary for detecting a faulty measurement.

NOMINAL EQUATION

The classical method using parity vector and chi-square distribution is examined to detect the faulty measurement. [10][11]

We examine our ability to detect the presence of a faulty measurement using one redundant measurement given our mixed ranging operations. To understand the capability, we make some simplifying assumptions on the measurements for ease of modeling: 1) There is only one measurement that is faulty (which results in a bias, B). 2) Measurement faults are equally likely. 3) All measurement noise has identical variance, σ^2.

Fault detection is based on hypothesis testing. A decision variable, D is constructed and tested against a threshold, Y. Thus, if D>Y, the presence of a faulty measurement is detected; otherwise no fault is detected. The decision variable D is obtained by the square of the magnitude of the parity vector:

$$D = p^T p$$

The performance of the test is characterized by the probability of false alarm P_{FA} and the probability of missed detection P_{MD}, which are defined as following respectively:

$$P_{FA} = P[D > Y \mid no\ fault]$$
$$P_{MD} = P[D < Y \mid with\ some\ fault]$$

In **Fig. 15,** V is the non-centrality parameter.

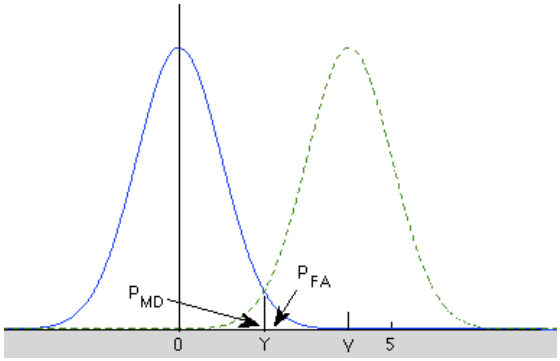

Figure 15: Definition of Probability of False Alarm and Missed Detection

If there are no faults, the expected value of the parity vector equals zero, and D/σ^2 has chi-square distribution with one degree of freedom. Thus, the probability of false alarm depends on the number of redundant measurements (only one redundant measurement is considered in our study), and is otherwise independent of geometry matrix G. Given the probability of false alarm, we are able to solve for the threshold-to-noise variance ratio, Y/σ^2 for all cases with the same amount of redundant measurements.

If there is a fault, the expected value of the parity vector is nonzero. As a result, D/σ^2 has non-central chi-square distribution with one degree of freedom and non-centrality parameter $V = (\frac{B^2}{\sigma^2})S_{ii}$, where S_{ii} is the i^{th} diagonal element of matrix S. $S = I_M - GG^*$.

EFFECT OF CLOCK OFFSET ERROR

Two different cases with one redundant measurement are discussed: 1) Two pseudo-range measurements and two true-range measurements from two stations; 2) Three pseudo-range measurements from three stations and previously determined clock offset. The effect of clock offset error for two cases is studied in this section.

In the first case, the results do not depend on the geometry of the stations. This is because each station, through a true-range and pseudo-range signal, allows a clock offset estimate. The relation between the probability of false alarm and missed detection for different values of $\frac{B}{\sigma}$ can be shown in **Fig. 16** below.

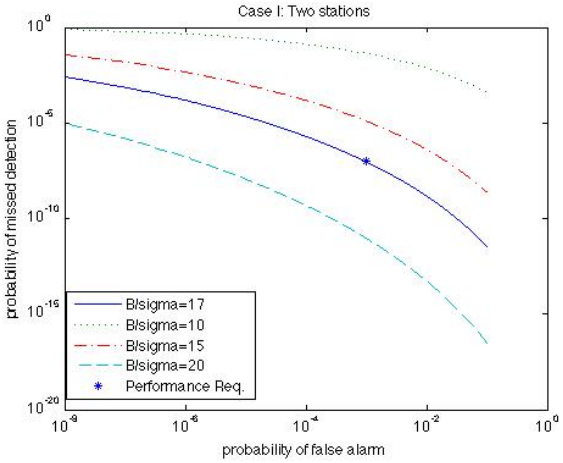

Figure 16: Case I, Probability of False Alarm vs. Missed Detection for Different Clock Offset Error

Given the probability of false alarm, the probability of missed detection increases as $\frac{B}{\sigma}$ decreases. Also, for a

fixed value of $\frac{B}{\sigma}$, the probability of missed detection decreases as the probability of false alarm increases.

If given the thresholds of probability of false alarm and missed detection: $P_{FA} = 0.001$, $P_{MD} = 10^{-7}$, which are indicated by the star sign in **Fig. 16** and **Fig. 17**, the minimal value of $\frac{B}{\sigma}$ that meets the requirements equals 17, that is, the clock offset bias error (from a fault) $B \geq 17\ \sigma$. The minimum bias that we can detect on clock offset is 17 times the standard deviation of the range measurement σ with the desired confidence and probability of false alarm. Hence, 10^{-7} integrity bound will result in a large inflation over the accuracy levels.

In the second case, the geometry matrix:

$$G = \begin{matrix} 1 & 0 & 1 \\ \cos\theta & \sin\theta & 1 \\ \cos\alpha & \sin\alpha & 1 \\ 0 & 0 & 1 \end{matrix}$$

where θ and α are angles between stations. The results depend on the geometry, that is, the relation between the P_{MD} and P_{FA} varies for different geometry. Given a specific geometry: $\theta = 60$ degrees and $\alpha = 30$ degrees, we can plot the P_{MD} vs. P_{FA} for different values of $\frac{B}{\sigma}$. In this case, the minimum bias, B, that we can detect on clock offset and satisfy the performance requirements is 19 σ, where σ is the standard deviation of the range measurement.

Fig. 17 below shows the result for this case, which is similar to the result obtained in the first case.

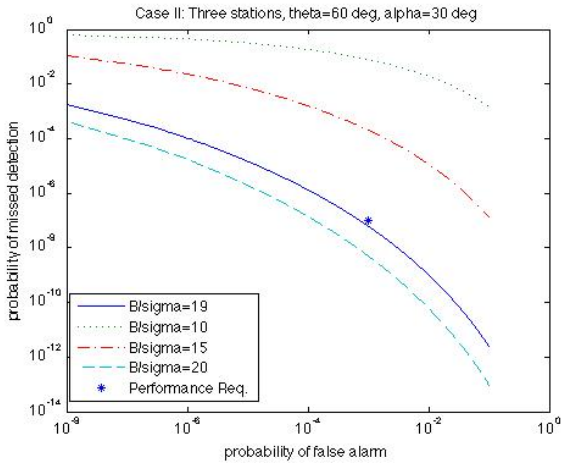

Figure 17: For a specific geometry, Probability of False Alarm vs. Missed Detection

If using the same thresholds: $P_{FA} = 0.001$, $P_{MD} = 10^{-7}$, and taking almost all geometry situations into consideration, the minimal value of $\frac{B}{\sigma}$ that can meet the performance requirements is represented in **Fig. 18** as a 3D plot which can be found below.

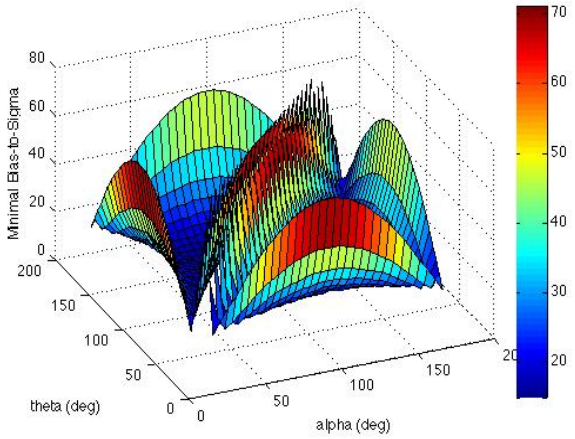

Figure 18: Minimal B/ σ for Different Geometry

Since the geometry matrix G is singular in the following cases: $\theta = \alpha$; $\theta = 0$ or 180 degrees; $\alpha = 0$ or 180 degrees, **Fig. 18** shows the results for all geometry situations from 10 to 170 degrees excluding the cases for $\theta = \alpha$. Along the $\theta = \alpha$ diagonal, $\frac{B}{\sigma}$ goes to infinity as G has rank 3. So as to not obscure the plot, we set it to "not a number" (NaN). The minimal value of $\frac{B}{\sigma}$ for different geometry achieves the minimum at $\theta = 60$ or 120 degrees, $\alpha = 120$ or 60 degrees. The minimum bias can be detected in this geometry is about 15 σ. Hence we see the challenge of using classical fault detection as high integrity only exists in the case of large biases relative to nominal errors.

6. CONCLUSIONS

Mixed positioning is desirable for APNT from an infrastructure and capacity perspective. With three measurements or more in the clock calibration mode, we are able to estimate the horizontal position of aircraft and clock offset.

Using the estimated clock offset as the previously determined in the clock-coasting mode, allows for the use of only two pseudo-range measurements to navigate the aircraft. This mixed positioning can allow APNT to maintain high system capacity while minimizing the needed number of ground stations. The mixed positioning can solve for an important problem for APNT: fewer terrestrial ground stations are visible to aircraft in terminal airspace where they are most needed due to accuracy and capacity requirements.

In this paper, we derived the error distribution for many different cases for mixed positioning. The key result is determining the error distribution of the clock offset after clock calibration is performed and how that error grows in

the clock coast phase. The results indicate a TCXO or better class oscillators should allow for a reasonable amount of coasting – reducing geometry needs and two-way interactions. This is especially true if the oscillator has been recently calibrated which should occur when GPS is available.

In the aircraft navigation, considering integrity is a must. In this paper, we focus on how to detect the faulty source using one redundant measurement and the effect of clock offset. The analysis shows that using classical receiver autonomous integrity monitoring (RAIM) techniques with one redundant measurement results in high inflation factor if integrity levels of 10^{-7} (with false alarm levels of 10^{-3}) are used. For the two cases we studied on, the detectable bias needs to be at least 15 times the standard deviation of the nominal error. Hence, use of classical RAIM with the limited geometry may be challenging. Examining more modern techniques such as multiple hypothesis solution separation and ways of gaining some integrity credit through more ground monitoring may improve integrity bounds. Ground monitoring of the DME ground station already exists and such an assumption is reasonable.

ACKNOWLEDGMENTS

The author would like to thank the FAA Navigation Services Directorate and APNT program for supporting this work and really thankful to Dr. Sherman Lo and Prof. Per Enge. This paper would not have been possible without their support.

DISCLAIMER

The views expressed herein are those of the authors and are not to be construed as official or reflecting the views of the United States Federal Aviation Administration or Department of Transportation.

REFERENCES

[1] M. Narins, et al., "Alternative Position, Navigation, and Timing -- The Need for Robust Radionavigation," Proceedings of the Royal Institute of Navigation NAV10, Westminster, London, UK, November-December 2010

[2] L. Eldredge, et al., "Alternative Positioning, Navigation & Timing (PNT) Study," International Civil Aviation Organisation Navigation Systems Panel (NSP), Working Group Meetings, Montreal, Canada, May 2011

[3] Sherman Lo, Per Enge "Assessing the Capability of Distance Measuring Equipment (DME) to Support Future Air Traffic Capacity", Submitted to Navigation: The Journal of the Institute of Navigation, 2011

[4] Sherman Lo, Per Enge, "Signal Structure Study for Passive Ranging System using Existing Distance Measuring Equipment (DME)" Proceedings of the Institute of Navigation International Technical Meeting, Newport Beach, CA, January 2012

[5] Sherman Lo, Benjamin Peterson, Dennis Akos, Mitch Narins, Robert Loh, Per Enge, "Alternative Position Navigation & Timing (APNT) Based on Existing DME and UAT Ground Signals" Proceedings of the Institute of Navigation GNSS Conference, Portland, OR, September 2011

[6] RTCA Special Committee 159, "Minimum Operational Performance Standards for Airborne Supplemental Navigation Equipment Using Global Positioning System (GPS)," Document No. RTCA/DO-208, 1991

[7] A. Trunzo, P. Benshoof, J. Amt, "The UHARS Non-GPS Based Positioning System," Proceedings of the ION GNSS 2011 Conference, Portland, OR September 2011.

[8] Michael Schnell, German Aerospace Center (DLR), "APNT – A New Approach Using LDACS1", Presentation at APNT Industry day, IEEE/AIAA Digital Avionics System Conference (DASC), October 2011

[9] J.R. Vig, "Quartz Crystal Resonators and Oscillators for Frequency Control and Timing: A Tutorial," US Army Electronics Technology and Devices Laboratory, For Monmouth, NJ, October 1991.

[10] Navigation System Integrity Monitoring Using Redundant Measurements, Mark A. Sturza, Litton Systems Inc., Woodland Hills, California, 1988

[11] Samuel P. Pullen, Boris S. Pervan, Bradford W. Parkinson, "A New Approach to GPS Integrity Monitoring Using Prior Probability Models and Optimal Threshold Search", Position Location and Navigation Symposium, 1994, IEEE.

[12] Olie Mancini, "Tutorial: Precision Frequency Generation Utilizing OCXO and Rubidium Atomic Standards with Applications for Commercial, Space, Military, and Challenging Environments", Given to IEEE Long Island Chapter, March 2004